

Felix A. Himmelstoss, Sergey Ryvkin

DC/DC Converter for Motor Drive - Concept, Design, and Feed-Forward Control

DOI 10.7305/automatika.54-3.380
UDK 681.532.5.015:621.314.5.072.2(621.383.51)
IFAC 4.3.1; 5.5.4

Original scientific paper

Solar photovoltaics is one of the most promising technologies for the non-carbon based electricity production. Power electronics is therefore necessary. In this paper a converter is analyzed which makes it possible to control the mean value of the output voltage, this is e.g. the voltage across a DC machine (and therefore the speed) from zero up to three times of the input voltage. The converter is also useful for charging batteries. The model of the drive, the design of the devices, the control features are discussed, feed-forward control based on solving the limit cycle is designed, some experimental results, and hints for the design are given.

Key words: Current control, DC/DC converter, Feed-forward control

DC/DC pretvarači za motorne pogone – koncept, dizajn i unaprijedno upravljanje. Solarni paneli jedni su od najznačajnijih sustava za proizvodnju električne energije koja se ne temelji na ugljenu. U te svrhe nužno je korištenje učinkive elektronike. U ovome radu analiziran je ispravljač koji omogućuje upravljanje srednjom vrijednosti izlaznog napona, tj. napona u odnosu na DC uređaj (stoga i upravljanje brzinom) u rasponu od nule pa do tri puta razine izlaznog napona. Ispravljač se također može koristiti za punjenje baterija. Model i dizajn uređaja zajedno sa sustavom upravljanja opisani su u radu. Prikazano je unaprijedno upravljanje temeljeno na rješavanju graničnih ciklusa, dani su eksperimentalni rezultati te su prikazane pojedinosti dizajniranja uređaja.

Ključne riječi: upravljanje strujom, DC/DC pretvarač, unaprijedno upravljanje

1 INTRODUCTION

One of the main causes of the change of climate is electricity production based on fossil (and short term) energy sources. Their increased demand, first of all of oil, will heighten concerns over the security of supplies [1, 2]. The current path must be changed. Tools for such change are energy revolution and low-carbon energy technologies. This means that the “green electronics” side must be taken. The “green electronics” involves two major technologies [3]. One is using renewable energy sources, e.g. wind energy, photovoltaics (PV), sea waves [4], and so on and transform them into electricity. The second one is to use the electrical energy as efficiently as possible by using highly efficient power electronics in power generation, power transmission/distribution, and end-user applications.

The most abundant energy resource on earth is solar energy. Direct conversion of sunlight into electricity in PV cells is one of the main technologies. Solar PV power has a particularly promising future. The IEA roadmap envisions that by 2050, PV will provide 11% of global electric-

ity production (4500 TWh per year) [2]. This level of PV will bring about, together with contributing to significant greenhouse gas emission reductions, substantial benefits in terms of security of energy supply and socio-economic development. To achieve this target will require cost reduction of the system components (PV modules, DC/AC inverters, cables, fittings and man-power) and increased conversion efficiency of the PV conversion, and the development of optimal technology.

The PV cell is an all-electrical device that produces electrical power directly from sunlight. The PV module that usually consists of around 36 or 72 cells connected in series, encapsulated in a structure made of e.g. aluminium, hasn't any moving parts. Therefore, its lifetime could be more than 25 years. However, the majority of the used PV modules has a light-to-electricity efficiency of no more than 15 % and a very large area for the production of the needed end-user application voltage is necessary. Second, the PV module generation capability may be reduced to (75 ~ 80) % of the nominal rate due to ageing.

A step-up-down DC/DC converter can change the out-

put voltage within a wide range even at a low value of the input voltage [1]. Such a converter can be a separate one, if the end-user application needs a DC voltage or is part of the power transmission between the PV module and a DC-AC grid side inverter, e.g. a multi-string one. The converter is equipped with power semiconductor switches, e.g. Insulated-Gate Bipolar Transistors (IGBTs) or field effect transistors (MOSFET) operating in switch mode with distinctly higher switching frequency.

The paper can be outlined as follows. Section 2 deals with the presented step-up-down converter. The function is explained, and the voltage stress of the semiconductor devices is calculated. Furthermore, a switched, and a non-linear model for a converter driving a DC machine are derived. Section 3 presents the approximate mathematical descriptions of the state variables for the two modes of the converter. Section 4 shows the control task formulation and considers a modulation design technique. The design result is the PWM control for the above mentioned drive system. Some practical control considerations, the generation of the set point and some measurements of the converter illustrate the features of the suggested control are presented in section 5. The paper is finished by the conclusion.

2 DC/DC CONVERTER

The basic converter is shown in Fig.1 [5] and consists of an inductor L , an active switch S , a capacitor C , and a passive switch D . The positive pole of the output voltage is the cathode of the diode. The machine is modelled by a voltage source U_q and an inductor L_A . Due to the additional capacitor C and the additional inductor L , the classical one-quadrant drive, which is only a step-down converter, is transferred into a step-up-down converter. The mean value of the output voltage \bar{U}_2 (the voltage across the diode, this is also the voltage across the armature terminals), with the duty ratio of the active switch d (the on-time of the active switch referred to the switching period) and neglecting the losses is the same as the well-known buck-boost converter.

The converter is a one-quadrant step-up step-down converter, which makes it possible to drive a DC motor in one direction; controlled braking is not possible with this circuit. For other concepts, control applications, and detail about the electrical machine refer to the references [6 till 9]. Figure 2 shows a two-quadrant converter developed from Fig. 1. The converter consists now of a half-bridge with two active and two passive switches and again one inductor and one capacitor as storage elements. Now both current directions are possible and therefore controlled braking with feeding back energy into the input source is achieved.

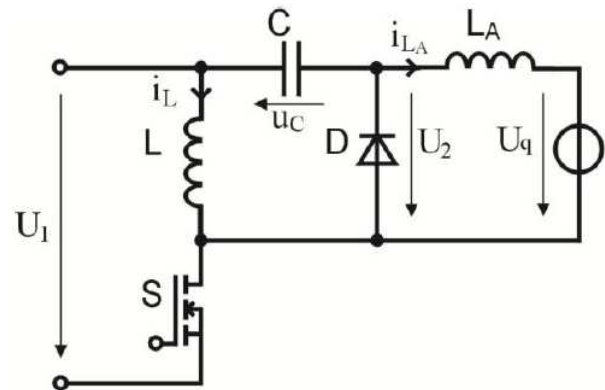


Fig. 1. One-quadrant step-up-down DC motor drive

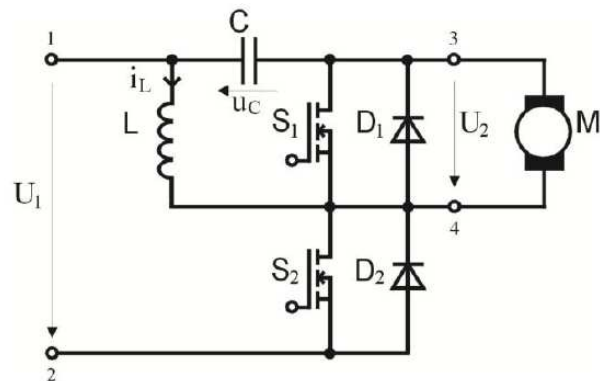


Fig. 2. Two-quadrant step-up-down DC motor drive

2.1 Basic Analysis

The basic analysis has to be done with idealized components (that means no parasitic resistors, no switching losses) and for the continuous mode in steady (stationary) state. A good way to start is to consider the voltage across the inductors.

As for the stationary case the absolute values of the voltage-time-areas of the inductors have to be equal (the voltage across the inductor has to be zero in the average), we can easily draw the shapes according to Fig. 3 and Fig. 4. (Here the capacitor is assumed so large that the voltages can be regarded constant during a pulse period.) Figure 3 shows the current through and the voltage across L . Of course the rate of rise of the current depends on the values of L and U_1 . Figure 4 shows the current through and the voltage across armature inductor L_A . Based on the equality of the voltage-time-areas in the stationary case (it should be mentioned that the source voltage is dependent on the speed, but is constant in the steady state case), it is

easy to give the transformation relationship for the source voltage U_q dependent on the input voltage U_1 and the duty ratio d . From Fig. 4 we get

$$(U_C + U_1 - U_q) \cdot d = (1 - d) \cdot U_q, \quad (1)$$

and from Fig. 3

$$U_1 \cdot d = (1 - d) \cdot U_C. \quad (2)$$

After a few steps we get the voltage transformation law

$$M = \frac{\bar{U}_2}{U_1} = \frac{U_q}{U_1} = \frac{d}{(1 - d)}. \quad (3)$$

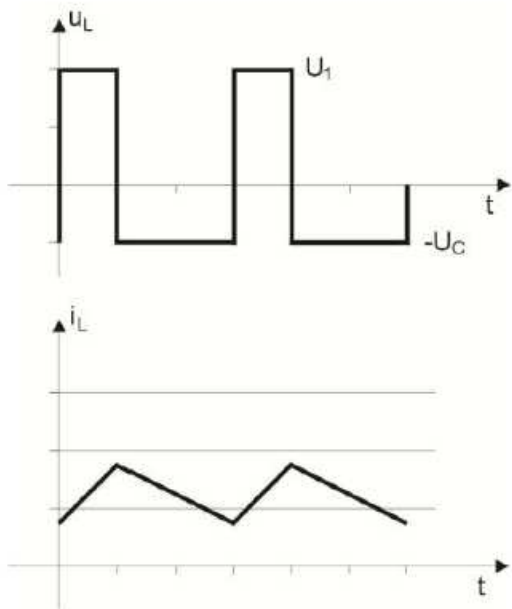


Fig. 3. Voltage across and current through the inductor L

Figure 5 shows the voltage transformation factor $M = \frac{U_q}{U_1}$ [the ratio of mean value of the output voltage of the converter (or the source voltage of the machine) to input voltage] in dependence on the duty cycle d . The converter is a step-up converter.

Neglecting all losses, the source voltage of the machine in steady case is equal to the mean value of the output voltage. Therefore, the speed of the motor (with C_E as voltage constant of the machine) is

$$n_0 = \frac{1}{C_E} \cdot \frac{d}{1 - d} \cdot U_1. \quad (4)$$

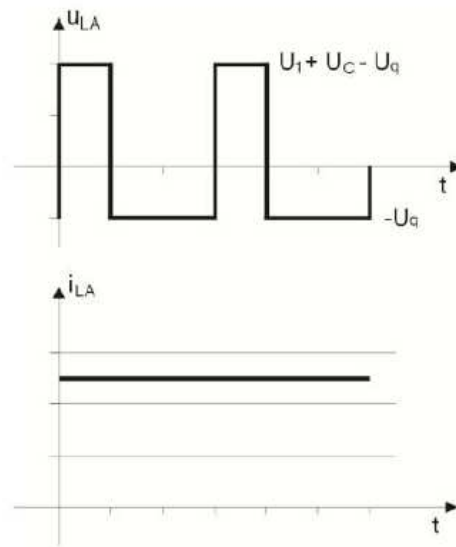


Fig. 4. Voltage across and current through the inductor L_A

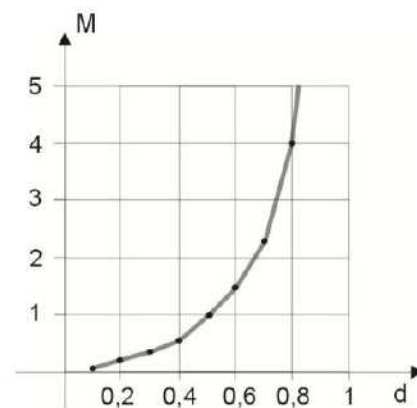


Fig. 5. Voltage transformation rate in dependence on the duty cycle

In the same manner a relationship for the current through the inductors can be derived based on the equality of the absolute values of the current-time-areas of the capacitor during on- and off-times of the active switch. From Fig. 6 we get

$$\bar{I}_L(1 - d) = I_{LA} \cdot d, \quad (5)$$

$$\bar{I}_L = I_{LA} \cdot \frac{d}{(1 - d)}. \quad (6)$$

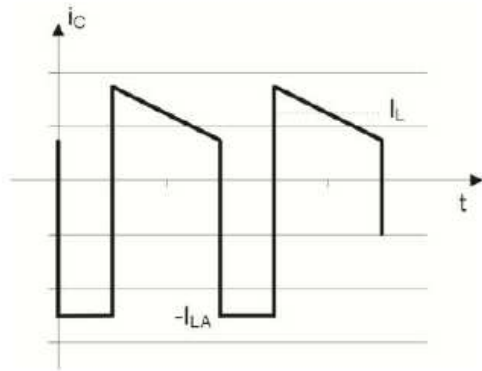


Fig. 6. Current through the capacitor C

For the dimensioning of the circuit, the voltage rates for the semiconductors are important. According to the on-state (*S* on, *D* off), the voltage across the switch *S* is

$$U_{S,max} = U_1 + U_C = U_1 + U_1 \frac{d}{(1-d)} = U_1 \frac{1}{(1-d)} \quad (7)$$

The same value occurs in the other state (*S* off, *D* on) across the diode

$$U_{D,max} = U_1 + U_C = U_1 \frac{1}{(1-d)} \quad (8)$$

2.2 Converter Model

For the DC motor the standard model based on [6] with constant field flux which can be assumed if a permanent magnet is employed or a constant excitation, is used. R_A is the armature resistance, L_A the armature inductance, C_T and C_E the motor constants for torque and source voltage, J the inertia and B the damping. The state variables are the inductor current i_L , the armature current i_A , the capacitor voltage u_C , and the speed n . The input variables are the input voltage u_1 , and the work load (load torque) t_{WL} . The fixed forward voltage of the diode (the diode is modeled as a fixed forward voltage V_{FD} and an additional voltage drop depending on the differential resistor of the diode R_D) is included as an additional vector. The parasitic resistances are the on-resistance of the active switch R_S , the series resistance of the coil R_L , the series resistor of the capacitor R_C , and the differential resistor of the diode R_D .

In continuous inductor current mode there are two states. In state one the active switch is turned on (or the first active switch is turned on in case of the two-quadrant drive) and the passive switch is turned off (or the second active

switch is turned off in case of the two-quadrant drive). Figure 7 shows this switching state one.

The state space equations are now

$$\frac{di_L}{dt} = \frac{-i_L(R_L + R_S) - i_{LA} \cdot R_S + u_1}{L}, \quad (9)$$

$$\frac{di_{LA}}{dt} = \frac{-i_L \cdot R_S - i_{LA}(R_{LA} + R_C + R_S) + u_C + u_1 - c_E \cdot n}{L_A} \quad (10)$$

$$\frac{du_C}{dt} = \frac{-i_{LA}}{C}, \quad (11)$$

$$\frac{dn}{dt} = \frac{c_T \cdot i_{LA} - t_{WL}}{2\pi J}. \quad (12)$$

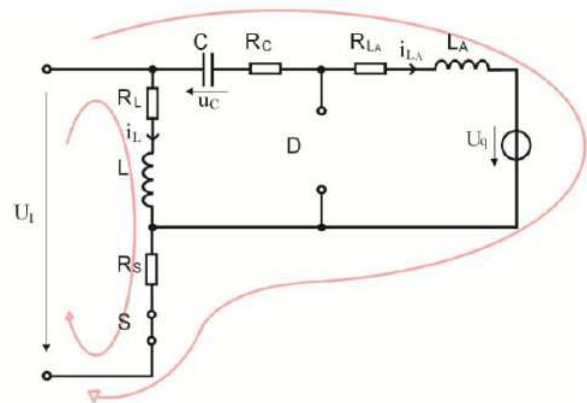


Fig. 7. Equivalent circuit for state one for the one-quadrant drive

In state two the active switch is turned off (or the first active switch is turned off and the second switch is turned on in case of the two-quadrant drive) and the passive switch is turned on. Fig. 8 shows this switching state two. The describing equations are

$$\frac{di_L}{dt} = \frac{-i_L(R_L + R_C + R_D) - i_{LA} \cdot R_D - V_{FD} - u_C}{L}, \quad (13)$$

$$\frac{di_{LA}}{dt} = \frac{-i_L \cdot R_D - i_{LA}(R_{LA} + R_D) - V_{FD} - c_E \cdot n}{L_A}, \quad (14)$$

$$\frac{du_C}{dt} = \frac{i_L}{C}. \quad (15)$$

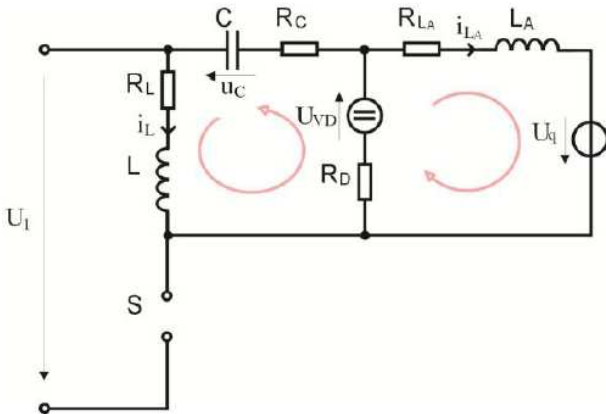


Fig. 8. Equivalent circuit for state two for the one-quadrant drive

The mechanical equation is the same as in state 1 (12).

When using two active switches in push-pull mode, the diode is shunted and V_{FD} can be set to zero. R_D is then the on-resistance of the second switch. Combining the two systems by the state-space averaging method leads to a model, which describes the drive in the mean. On condition that the system time constants are large compared to the switching period, we can combine these two sets of equations.

Weighed by the duty ratio, the combination of the two sets yields to

$$\frac{d}{dt} \begin{pmatrix} i_L \\ i_{LA} \\ u_C \\ n \end{pmatrix} = \begin{bmatrix} -[d \cdot R_S + (1-d) \cdot (R_C + R_D) + R_L] & -[d \cdot R_S + (1-d) \cdot R_D] & \frac{(d-1)}{L} & 0 \\ -[d \cdot R_S + (1-d) \cdot R_D] & -[d \cdot (R_C + R_S) + R_{LA} + (1-d) \cdot R_D] & \frac{d}{L_A} & -\frac{C_E}{L_A} \\ \frac{(1-d)}{C} & \frac{-d}{L_A} & 0 & 0 \\ 0 & \frac{C}{2\pi J} & 0 & 0 \end{bmatrix} \cdot \begin{pmatrix} i_L \\ i_{LA} \\ u_C \\ n \end{pmatrix} + \begin{bmatrix} \frac{d}{L} & 0 \\ \frac{d}{L_A} & 0 \\ 0 & 0 \\ 0 & \frac{1}{2\pi J} \end{bmatrix} \cdot \left(u_1 \right) + \begin{pmatrix} \frac{d-1}{L} \\ \frac{d-1}{L_A} \\ 0 \\ 0 \end{pmatrix} \cdot V_{FD} \quad (16)$$

By the given system of equations the dynamic behavior of the idealized converter is described correctly in the average, thus quickly giving us a general view of the dynamic behavior of the converter. The superimposed ripple (which appears very pronounced in the coils) is of no importance for qualifying the dynamic behavior. This model is also appropriate as large-signal model, because no limitations with respect to the signal values have been made. Linearizing this system around the operating point enables us to calculate transfer functions for constructing Bode plots

and to use the linear control theory. The results are shown in [10].

3 MATHEMATICAL DESCRIPTION OF THE STATE VARIABLES

In this section a second more mathematical way to look at the converter and the machine is described here. All losses are neglected except the armature resistor of the machine. This concept is useful when a small capacitor is used. The standard model DC motor [7, 9] with constant field flux, which can be assumed, if a permanent magnet is employed, or a constant excitation is used

$$\begin{aligned} di_A/dt &= (-R_A i_A - C_E n + u_A)/L_A, \\ dn/dt &= (C_M i_A - T_{load})/J \end{aligned} \quad (17)$$

where u_A is the motor input voltage, C_M , C_E are the motor constants for torque and source voltage, J is the inertia, T_{load} is the load torque.

By using the two-position switch S it is possible to form an average voltage value on the DC motor winding that is needed for solving the control problem in the switched mode. These two switch positions cause two modes of this drive: switch-on one and switch-off one. Each switching structure has two loops and its features.

3.1 Switch on mode

The input motor voltage u_A is the sum of the converter input voltage U_1 and the capacitor voltage u_C (Fig. 2). The current through the capacitor discharges it and therefore the voltage across it will be reduced. The behaviour of the DC drive can be described by the following equation

$$u_1 = \frac{1}{C} \int i_A^k dt + R_A i_A^k + L_A \frac{di_A^k}{dt} + C_E n, \quad (18)$$

where all variables in this mode have the upper index k. The solution of this equation describes the changing of the load current i_A and the capacitor voltage u_C in this mode

$$i_A^k = C e^{-\lambda t} [(C^2 \omega_1 - C^1 \lambda) \cos(\omega_1 t) - (C^2 \lambda + C^1 \omega_1) \sin(\omega_1 t)] \quad (19)$$

$$u_C^k = (u_1 - C_E n) + e^{-\lambda t} [C^1 \cos(\omega_1 t) + C^2 \sin(\omega_1 t)]. \quad (20)$$

where $\lambda = R_A/(2L_A)$; $\omega^2 = 1/(L_A C)$, $\omega_1 = \sqrt{\omega^2 - \lambda^2}$, C^1 and C^2 are the constants of integration according

$$\begin{aligned} C^1 &= U_C^{0\ k} - (u_1 - C_{En}), \\ C^2 &= \frac{1}{\omega_1} \left\{ \frac{I_A^{0\ k}}{C} + \lambda [U_C^{0\ k} - (u_1 - C_{En})] \right\}. \end{aligned} \quad (21)$$

where $I_A^{0\ k}$ is the motor current starting condition, $U_C^{0\ k}$ is the capacitor starting condition.

At the same time, in the second loop the inductor L is connected to the input voltage U_1 (Fig. 3), the inductor current i_L is increasing, and the inductor accumulates energy

$$u_1 = L(di_L^k/dt). \quad (22)$$

The solution of this equation describes the changing of the inductor current i_L in this mode

$$i_L^k = (u_1/L)t + I_L^{0\ k} \quad (23)$$

where $I_L^{0\ k}$ is the inductor current starting condition.

3.2 Switch off mode

In this mode the motor is free-wheeling, as there is no voltage across the armature (Fig. 4). The behavior is described as

$$0 = R_A i_A^{k+1} + L_A \frac{di_A^{k+1}}{dt} + C_{En} \quad (24)$$

the variable in this mode has the upper index $(k+1)$.

The solution of this equation describes the changing of the load current i_A in this mode

$$i_A^{k+1} = -(C_{En}/R_A) + C^3 e^{-\frac{R_A}{L_A}t}, \quad (25)$$

where C^3 is the constant of integration

$$C^3 = I_A^{0\ k+1} + (C_{En}/R_A), \quad (26)$$

where $I_A^{0\ k+1}$ is the motor current starting condition.

At the same time the second loop is a LC tank set up by the inductor L and the capacitor C (Fig. 5). The energy accumulated in the inductor L is going to the capacitor C. The initial condition is omitted in (27), because the solution is done according to the second order differential equation. Its voltage is increasing

$$0 = \frac{1}{C} \int i_L^{k+1} dt + L \frac{di_L^{k+1}}{dt}. \quad (27)$$

The solution of this equation describes the changing of the capacitor voltage u_C and of the inductor current i_L in this mode

$$u_C^{k+1} = (C^4 \cos \omega_2 t + C^5 \sin \omega_2 t), \quad (28)$$

$$i_L^{k+1} = C\omega_2 (C^5 \cos \omega_2 t - C^4 \sin \omega_2 t), \quad (29)$$

where $\omega_2^2 = 1/(LC)$, C^4 and C^5 are the constants of integration

$$C^4 = U_C^{0\ k+1}, \quad C^5 = I_L^{0\ k+1}/(C\omega_2), \quad (30)$$

where $U_C^{0\ k+1}$ is the capacitor starting condition and $I_L^{0\ k+1}$ is the inductor current starting condition.

4 FEED-FORWARD CONTROL DESIGN

The control goal is to make the motor current equal to the reference value i_{Az} by using the switching mode. However, solving this problem is associated with the capacitor voltage value. It must be designed in such a way that the modulation control guarantees a stable average value of the motor current within the modulation period.

From a control viewpoint the solution is to find the limit cycle in this system. The cycle parameters can be found under the condition that the control variable on the $(k+1)$ -th cycle end is equal to those at the beginning of the k -th cycle. And the variables: the load current i_A , the capacitor voltage u_C and the inductor current i_L cannot be discontinuous at the border between the k -th cycle and the $(k+1)$ -th one.

The existence conditions of such a limit cycle are the following:

- for motor current

$$-C_{En}/R_A + C^3 e^{-\frac{R_A}{L_A}t^{k+1}} = I_A^{0\ k} \quad (31)$$

$$i_{Az} = \frac{1}{t^k + t^{k+1}} \left\{ \int_0^{t^k} i_A^k dt + \int_0^{t^{k+1}} i_A^{k+1} dt \right\} \quad (32)$$

- for capacitor voltage

$$[C^4 \cos(\omega t^{k+1}) + C^5 \sin(\omega t^{k+1})] = U_C^{0\ k} \quad (33)$$

- for inductor current

$$C\omega_2 [C^5 \cos(\omega_2 t^{k+1}) - C^4 \sin(\omega_2 t^{k+1})] = I_L^{0\ k} \quad (34)$$

where t^k and (t^{k+1}) are the durations of the switch-on and switch-off period accordingly.

Let us rewrite the above-mentioned existence conditions (31)-(34) by using the equations (19)-(23), (25), (26), (30):

$$\begin{aligned} & (u_1 - C_{EN}) \{1 - e^{-\lambda t^k} [\cos(\omega_1 t^k) + \frac{\lambda}{\omega_1} \sin(\omega_1 t^k)]\} * \\ & * \cos(\omega_2 t^{k+1}) + \frac{1}{C\omega_2} \frac{u_1}{L} t^k \sin(\omega_2 t^{k+1}) + \\ & + \frac{e^{-\lambda t^k}}{\omega_1 C} \sin(\omega_1 t^k) \cos(\omega_2 t^{k+1}) I_A^{0k} + \{e^{-\lambda t^k} [\cos(\omega_1 t^k) + \\ & + \frac{\lambda}{\omega_1} \sin(\omega_1 t^k)] \cos(\omega_2 t^{k+1}) - 1\} U_C^{0k} + \\ & + \frac{1}{C\omega_2} \sin(\omega_2 t^{k+1}) I_L^{0k} = 0 \end{aligned} \quad (35)$$

$$\begin{aligned} & -C\omega_2 (u_1 - C_{EN}) \{1 - e^{-\lambda t^k} [\cos(\omega_1 t^k) + \\ & + \frac{\lambda}{\omega_1} \sin(\omega_1 t^k)]\} \sin(\omega_2 t^{k+1}) + \\ & + \frac{u_1}{L} t^k \cos(\omega_2 t^{k+1}) - \frac{e^{-\lambda t^k} \omega_2}{\omega_1} \sin(\omega_1 t^k) * \end{aligned}$$

$$\begin{aligned} & * \sin(\omega_2 t^{k+1}) I_A^{0k} - C\omega_2 e^{-\lambda t^k} [\cos(\omega_1 t^k) + \\ & + \frac{\lambda}{\omega_1} \sin(\omega_1 t^k)] \sin(\omega_2 t^{k+1}) U_C^{0k} + \\ & + [\cos(\omega_2 t^{k+1}) - 1] I_L^{0k} = 0 \end{aligned} \quad (36)$$

$$\begin{aligned} & -(1 - e^{-\frac{R_A}{L_A} t^{k+1}}) \frac{C_{EN}}{R_A} - \frac{\omega_2^2}{\omega_1 C} e^{-(\lambda t^k + \frac{R_A}{L_A} t^{k+1})} * \\ & * (u_1 - C_{EN}) \sin(\omega_1 t^k) + \\ & + \{e^{-(\lambda t^k + \frac{R_A}{L_A} t^{k+1})} [\cos(\omega_1 t^k) - \\ & - \frac{\lambda}{\omega_1} \sin(\omega_1 t^k) - 1]\} I_A^{0k} + \\ & + e^{-(\lambda t^k + \frac{R_A}{L_A} t^{k+1})} \frac{\omega_2^2 C}{\omega_1} \sin(\omega_1 t^k) U_C^{0k} = 0 \end{aligned} \quad (37)$$

$$\begin{aligned} i_{Az} = & \frac{1}{t^k + t^{k+1}} \{C e^{-\lambda t^k} [\frac{\lambda}{\omega_1} \sin(\omega_1 t^k) + \\ & + \cos(\omega_1 t^k) - 1] (u_1 - C_{EN}) + \\ & + \frac{C_{EN}}{R_A} \{-t^{k+1} + (-\frac{L_A}{R_A}) (e^{-\frac{R_A}{L_A} t^{k+1}} - 1)\} + \\ & + \frac{e^{-\lambda t^k} \omega_2^2 C}{\omega_1} (u_1 - C_{EN}) \sin(\omega_1 t^k) * \\ & * (-\frac{L_A}{R_A}) (e^{-\frac{R_A}{L_A} t^{k+1}} - 1) + \\ & + \{e^{-\lambda t^k} \frac{\sin(\omega_1 t^k)}{\omega_1} + \\ & + [\cos(\omega_1 t^k) - \frac{\lambda}{\omega_1} \sin(\omega_1 t^k)] e^{-\lambda t^k} * \\ & * (-\frac{L_A}{R_A}) (e^{-\frac{R_A}{L_A} t^{k+1}} - 1)\} I_A^{0k} + \\ & + \{C e^{-\lambda t^k} [\frac{\lambda}{\omega_1} \sin(\omega_1 t^k) + \cos(\omega_1 t^k) - \\ & - 1] - \frac{e^{-\lambda t^k} \omega_2^2 C}{\omega_1} \sin(\omega_1 t^k) (-\frac{L_A}{R_A}) * \\ & * (e^{-\frac{R_A}{L_A} t^{k+1}} - 1)\} U_C^{0k} \} \end{aligned} \quad (38)$$

The joint solution of the equations (35)-(38) renders it possible to receive the parameters of the limit cycles of the load current, the inductor one, the capacitor voltage, and the duration of the switch-on period as the functions of the switch-off period. These very complicated equations could

be simplified, if we take into account that today the modulation frequency is very high, e.g. more than some ten kHz. In this case the modulation period is very small and the sinus function is equal to its argument, the cosine function is equal to one and the exponential function is equal to the sum of one and its argument.

Using these assumptions and a new variable d - the duty ratio of the switch S that is the switch-on time referred to the switching period - it is possible to receive the simplified equation system describing the limit cycle:

$$I_A^{0k} d + (1 - d) I_L^{0k} = 0, \quad (39)$$

$$(u_1/L)d - C\omega_2^2(1 - d)U_C^{0k} = 0, \quad (40)$$

$$\begin{aligned} & -(1 - d)C_{EN}/L_A - \omega_2^2(u_1 - C_{EN})d/C - \\ & - \lambda I_A^{0k} d + \omega_2^2 C \omega_1 U_C^{0k} d = 0 \end{aligned}, \quad (41)$$

$$C\lambda(u_1 - C_{EN})d + I_A^{0k} + C\lambda U_C^{0k} d = i_{Az}. \quad (42)$$

5 PRACTICAL CONSIDERATIONS

5.1 Generation of the inductor current set point value

Charging a battery or driving a motor in torque modus implies that the reference value is the load current and thus leads to the reference value for the inductor current

$$\bar{I}_L^* = I_{LA} \cdot \frac{U_q}{U_1}. \quad (43)$$

By including the resistors this reference value can be calculated more exactly (feed-forward control) or it can be calculated by an additional controller (feedback-control).

Controlling the speed of the motor affords an outer speed loop which generates the reference value of the inner current loop (the inner current loop controls the current of the converter and only indirectly the current of the motor).

When using a solar generator (or other generators with an optimal power point, like fuel cells, thermoelectric generators) as input source it is useful to control the input power according to a maximum power point tracker or a maximum power algorithm. Neglecting the losses the power at the optimum point must be the same as the output of the converter

$$U_{1,opt} \cdot I_{1,opt} = U_q \cdot I_{LA}. \quad (44)$$

For battery charging one gets the maximum load (charging) current according to

$$I_{LA,max} = \frac{U_{1,opt} \cdot I_{1,opt}}{U_q}, \quad (45)$$

and therefore the reference value for the hysteresis controller according to

$$\bar{I}_L^* = I_{1,opt} \frac{U_{1,opt} + U_q}{U_q}. \quad (46)$$

Here U_1 is the real input voltage and $U_{1,opt}$ the optimum input voltage according to the maximum power point (the value is generated by the maximum power point tracker). This reference value forces the system to the maximum input power.

5.2 Converter

The experimental results of the DC drive fed by the proposed step-up-down converter by the duty ratios of 0,34, 0,5 and 0,66 are presented in Figures 9 - 11, correspondingly. On these figures the horizontal time scale is $4 \mu s/div$. The variables are (up to down) the switch control signal (generated by the arbitrary pulse generator or by the modulator) (blue), the current through the machine (violet and nearly constant), the current through the inductor (turquoise and triangular shaped), and the voltage across the active switch (green).

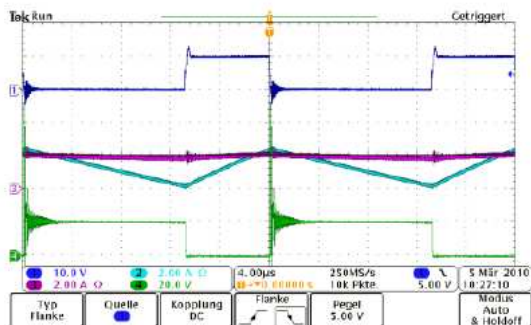


Fig. 9. Control signal of the active switched (blue), motor current (violet), inductor current (turquoise) and voltage across the active switch (green) by a duty ratio of 0.34

6 CONCLUSION

A novel step-up-down DC/DC converter is presented and analyzed from the control viewpoint. An additional simple LC-tank of the converter now makes it possible to generate a mean voltage across the output (e.g. the motor terminals), which value can not only be lower than the input voltage, but also higher, too. This is especially useful,

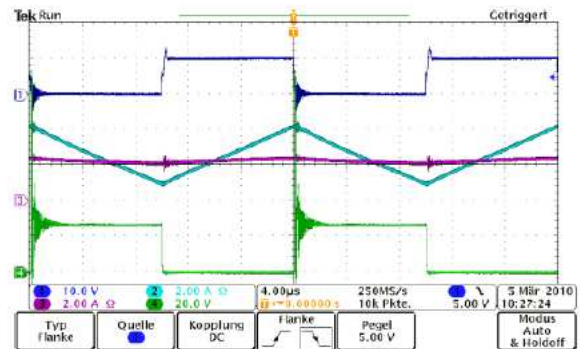


Fig. 10. Control signal of the active switched (blue), motor current (violet), inductor current (turquoise) and voltage across the active switch (green) by a duty ratio of 0.5

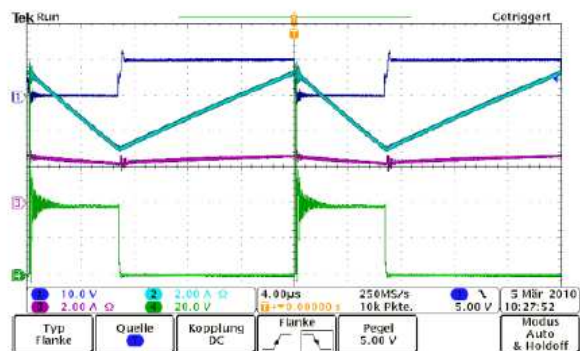


Fig. 11. Control signal of the active switched (blue), motor current (violet), inductor current (turquoise) and voltage across the active switch (green) by a duty ratio of 0.66

when only low input voltages are available. The proposed control solution is based on the voltage modulation. It is shown that in such a switching system there is a limit cycle that can be used for the open loop control design. The preliminary experimental results that have been carried out have confirmed the serviceability of such a control algorithm. From the control point of view the time constants are quite different: there is a large time constant caused by the mechanical inertia and due to the armature inductivity, a smaller, but still much higher one, compared to the time constant generated by the converter. Cascade control with a slow motion and a fast converter controller is therefore useful. The open and close loop controls and the influence of small parameter values of the converter will be studied in the future. The promising research directions are the design of a two quadrant DC-DC converter on the basis

of this converter and also of a three-phase voltage source inverter.

REFERENCES

- [1] F. Blaabjerg, F. Iov, T. Kerekes and R. Teodorescu, "Trends in power electronics and control of renewable energy systems," in *Proc. 14th International Power Electronics and Motion Control Conference, EPE-PEMC 2010*, pp. K-1 – K-19, Ohrid, Macedonia, 2010.
- [2] IEA-International Energy Agency; "Technology roadmaps - solar photovoltaic energy"; 2010.
- [3] H. Ohashi, "Role of green electronics in low carbonated society toward 2030," *Proc. 14th International Power Electronics and Motion Control Conference, EPE-PEMC 2010*, pp. K-20 – K-25, Ohrid, Macedonia, 2010.
- [4] M. Kazmierkowski and M. Jasunski, "Power electronics for renewable sea wave energy," in *Proc. 12th International Conference on Optimization of Electrical and Electronic Equipment, OPTIM 2010*, pp. 4-9, Brasov, Romania, 2010.
- [5] F. Himmelstoss, "Ein- und Zweiquadrantenstellglieder," *Austrian patent AT 507203 B1* filed 2008.10.30, 2008.
- [6] N. Mohan, T. Undeland and W. Robbins, *Power Electronics, Converters, Applications and Design*, 3rd ed., placeStateNew York: W. P. John Wiley & Sons, 2003.
- [7] I. Boldea and L. Tutelea, *Electric Machines: Steady State, Transients, and Design with MATLAB*, placeCityBoca Raton, StateFL: CRC Press Taylor and Francis Group, 2010.
- [8] F. Zach, *Power Electronics*, in German: *Leistungselektronik*, 4th edition, Wien: Springer, 2010.
- [9] W. Leonhard, "Control of electrical drive," 3rd ed., CityplaceSpringer-Verlag, StateBerlin,
- [10] F. Himmelstoss, Y. Flicker and M. Rabl, "A simple two-quadrant DC motor controller," in *Proc. 12th International Conference on Optimization of Electrical and Electronic Equipment, OPTIM 2010*, pp. 576-581, Brasov, Romania, 2010.
- [11] S. Ryvkin, and E. Palomar Lever, *Sliding Mode Control for Synchronous Electric Drives*, Balkema: CRC Press, 2011.
- [12] S. Ryvkin, S. and F. A. Himmelstoss, "Feedforward Control for Novel Photovoltaic DC/DC Converter," *Proceedings Electrical Drives and Power Electronics EDPE'2011*, The High Tatras, Stare Lesna, Sept. 28-30, 2011, pp. 194-199, ISBN: 978-80-553-0734-3.



Felix A. Himmelstoss was born in 1956 in Mödling, Austria. He received the Dipl.-Ing. and Dr. degrees from Technical University of Vienna, in 1981 and 1990, respectively. Since 1982 he has been working on different projects for Austrian companies developing power supplies and electrical drives. He is author/coauthor of numerous technical and scientific papers and patents. Dr. Himmelstoss is professor and head of the Energy and Industrial Electronics department of the University of Applied Science Technikum Wien.



Sergey Ryvkin first graduated with high honors as an engineer from the Moscow Institute for Aviation Engineering (Technical University), after which he gained his PhD degree from the Institute of Control Sciences (USSR Academy of Science) in Moscow and was awarded a DSc from the Supreme Certifying Commission of Russian Ministry of Education and Science in Moscow.

He is currently a professor at Moscow Power Engineering Institute (Technical University) and a main researcher at the Laboratory of Adaptive Control Systems for Dynamic objects at the Trapeznikov Institute of Control Sciences from the Russian Academy of Sciences. His lines of research are application of the sliding mode technique to control of electrical drives and power systems and to their parameter observation. Prof. Ryvkin holds six patents and published two monographs, five textbooks and more than 130 technical papers in international journals and conference proceedings. He is a full member of the Russian Academy of Electrotechnical Sciences and an IEEE senior member.

AUTHORS' ADDRESSES

Prof. Felix A. Himmelstoss, Ph.D.

University of Applied Science Technikum Wien, Vienna, Austria

email: Felix.himmelstoss@technikum-wien.at

Prof. Sergey Ryvkin, Ph.D.

Trapeznikov Institute of Control Sciences of Russian Academy of Sciences

Profsoyuznaya ul. 65, 117997, Moscow, Russia

email: rivkin@ipu.ru

Received: 2012-10-08

Accepted: 2012-11-07